Ca^{2+} Entry-Dependent Inactivation of L-Type Ca Current: A Novel Formulation for Cardiac Action Potential Models

Yuji Hirano and Masayasu Hiraoka
Department of Cardiovascular Diseases, Medical Research Institute, Tokyo Medical and Dental University, 1-5-45, Yushima, Bunkyo-ku, Tokyo 113-8510, Japan

ABSTRACT Cardiac L-type Ca current ($I_{Ca,L}$) is controlled not only by voltage but also by Ca^{2+}-dependent mechanisms. Precise implementation of $I_{Ca,L}$ in cardiac action potential models therefore requires thorough understanding of intracellular Ca^{2+} dynamics, which is not yet available. Here, we present a novel formulation of $I_{Ca,L}$ for action potential models that does not explicitly require the knowledge of local intracellular Ca^{2+} concentration ($[Ca^{2+}]_i$). In this model, whereas $I_{Ca,L}$ is obtained as the product of voltage-dependent gating parameters (d and f), Ca^{2+}-dependent inactivation parameters (f_{Ca}: $f_{Ca\text{-}entry}$ and $f_{Ca\text{-}SR}$), and Goldman-Hodgkin-Katz current equation as in previous studies, f_{Ca} is not a instantaneous function of $[Ca^{2+}]_i$ but is determined by two terms: onset of inactivation proportional to the influx of Ca^{2+} and time-dependent recovery (dissociation). We evaluated the new $I_{Ca,L}$ subsystem in the framework of the standard cardiac action potential model. The new formulation produced a similar temporal profile of $I_{Ca,L}$ as the standard, but with different gating mechanisms. Ca^{2+}-dependent inactivation gradually proceeded throughout the plateau phase, replacing the voltage-dependent inactivation parameter in the LRd model. In typical computations, f declined to ~0.7 and $f_{Ca\text{-}entry}$ to ~0.1, whereas deactivation caused fading of $I_{Ca,L}$ during final repolarization. These results support experimental findings that Ca^{2+} entering through $I_{Ca,L}$ is essential for inactivation. After responses to standard voltage-clamp protocols were examined, the new model was applied to analyze the behavior of $I_{Ca,L}$ when action potential was prolonged by several maneuvers. Our study provides a basis for theoretical analysis of $I_{Ca,L}$ during action potentials, including the cases encountered in long QT syndromes.

INTRODUCTION

Voltage-dependent L-type Ca channels ($I_{Ca,L}$) play vital roles for cardiac functions, including pacemaker activity in nodal cells, trigger for Ca^{2+}-induced Ca^{2+} release (CICR), and control of cardiac contractility (Bers and Perez-Reyes, 1999). $I_{Ca,L}$ also contributes to maintenance of the plateau or elongated depolarization of cardiac action potentials. Because $I_{Ca,L}$ is important to our understanding of cardiac functions in physiological as well as pathological conditions, mechanisms of its modulation have been studied extensively (McDonald et al., 1994).

One outstanding feature of $I_{Ca,L}$ is that it is inactivated not only by voltage but also by Ca^{2+}, the channel's own charge carrier (Eckert and Chad, 1984; Kass and Sanguinetti, 1984). Although these two different inactivation mechanisms have been known for a long time, precise mechanisms that control $I_{Ca,L}$ during action potentials have remained uncertain, including the relative contributions of the two inactivation mechanisms. Recently, however, several studies demonstrated that Ca^{2+} entering the cell through $I_{Ca,L}$ played predominant roles during the inactivation process of cardiac action potential (Linz and Meyer, 1998; Alseikhan et al., 2002).

We now have various types of models for cardiac action potentials. In most models, inactivation is mainly the result of a voltage-dependent process, with only a minor part for $[Ca^{2+}]_i$-mediated modulation. One reason for this underestimation of the role of Ca^{2+} may result because experimental data utilized for the computational models did not always discriminate two different inactivation mechanisms explicitly. Furthermore, due to the complicated nature of intracellular Ca^{2+} dynamics, modeling of CICR has often been implemented in a highly schematized or simplified style.

Recent studies have increasingly demonstrated the importance of local Ca^{2+} dynamics in cardiac functions. For example, studies on Ca^{2+} sparks and the "local control theory" implies distinct local Ca^{2+} signals in restricted space (reviewed in Wier and Balke, 1999). Several studies indicate the existence of a subcellular "fuzzy" space where concentration of ions may reach high levels. Also, studies on Ca^{2+}-dependent inactivation suggested direct interaction between Ca^{2+} ions entering through the channel and calmodulin that is constituently tethered to the channel protein (Zuhlke et al., 1999; Peterson et al., 1999). Thus, whereas modeling with detailed intracellular Ca^{2+} dynamics is necessary, there are many phenomena to be quantified before it can be implemented into a cardiac action potential model. Realistic modeling of the intracellular organization of Ca^{2+} and its effects on function should handle multiple cytosolic Ca^{2+} compartments, and may require development of higher resolution measurement techniques for imaging functional structures. Despite these obstacles, we do have

Submitted April 11, 2002, and accepted for publication August 29, 2002.
Address reprint requests to Yuji Hirano, MD, PhD, Dept. of Cardiovascular Diseases, Medical Research Institute, Tokyo Medical and Dental University, 1-5-45, Yushima, Bunkyo-ku, Tokyo 113-8510, Japan. Tel.: 81-3-5803-5830; Fax: 81-3-5684-6295; E-mail: hirano.card@mri.tmd.ac.jp.

0006-3495/03/01/696/13 $2.00

several important experimental and theoretical insights into the dynamics of Ca^{2+} release. Clearly, incorporation of these insights into cardiac action potential models is an important way to advance our understandings of cardiac function.

In this study, we employed an alternative approach. We present a novel formulation of Ca^{2+}-dependent inactivation, based on a simple assumption that does not require detailed knowledge of intracellular Ca^{2+} dynamics. Our results support experimental findings that Ca^{2+} entered through $I_{Ca,L}$ largely determine the inactivation process, and provide a basis for further theoretical analysis of $I_{Ca,L}$ during action potentials, including those encountered during long QT syndromes.

METHODS

Model equations

We started the computational study of Ca^{2+} entry-dependent inactivation using our locally written ventricular action potential models, and obtained essentially identical results with this report (Hirano and Hiraoka, 2001). Those models were based on the model proposed by DiFrancesco and Noble (1985), with several modifications to represent guinea-pig ventricular action potentials (Nakajima et al., 1999).

In this paper, we use the Luo-Rudy Phase II model as the control action potential model, based on the C++ source code downloaded from the research section of http://www.cwru.edu/med/CBRTC (Clancy and Rudy, 2001). This version of the Luo-Rudy dynamic model (referred to as the LRd model) has been revised several times since the original version (Luo and Rudy, 1994) was published, including the formulation of I_{Kr} and I_{Ks} current (Zeng et al., 1995; Viswanathan et al., 1999) and the on-off dynamics of Ca^{2+}-induced Ca^{2+}-release (Faber and Rudy, 2000). The program was modified as described below, keeping the essential part for the computation untouched. These included an adaptive time step method for integration. When the model was in voltage clamp mode (Fig. 6–8), however, time step interval was assigned with a fixed value of 0.002 ms. The C++ source code was compiled using Microsoft Visual C++ (ver. 6) and executed on a Pentium-III based personal computer. Numerical results were written in ASCII files, and were visualized using Microcal Origin (ver. 7.0J).

RESULTS

Ca^{2+} entry-dependent inactivation of L-type Ca channel

Recent observations on Ca^{2+}-dependent inactivation of $I_{Ca,L}$ indicate that Ca^{2+} entering through the channel pore directly interacts with calmodulin constituently tethered to an IQ motif (Peterson et al., 1999; Zuhlke et al., 1999). The most simple formulation of this effect might be that transition of channels into the Ca^{2+}-inactivated state is proportional to the amount of Ca^{2+} (charges) entering through the channel openings.

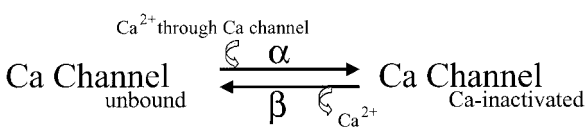

We define a Ca^{2+}entry-dependent inactivation property with a parameter $f_{Ca\text{-}entry}$ as the proportion of unbound Ca channels (Unbound / (Unbound + Ca-inactivated)). Changes in $f_{Ca\text{-}entry}$ ($\Delta f_{Ca\text{-}entry}$) were determined by a term proportional to Ca^{2+} influx through the channel ($-\alpha \times I_{Ca,L}$) and time-dependent recovery which takes place in the proportion of Ca^{2+}-inactivated channels ($\beta \times (1 - f_{Ca\text{-}entry})$):

$$\Delta f_{Ca\text{-}entry} = -\alpha \times I_{Ca,L} \times \Delta t + \beta \times (1 - f_{Ca\text{-}entry}) \times \Delta t$$

or in the form of a differential equation:

$$\frac{df_{Ca\text{-}entry}}{dt} = -\alpha \times I_{Ca,L} + \beta \times (1 - f_{Ca\text{-}entry}). \quad (1)$$

$I_{Ca,L}$ is now computed by the Goldman-Hodgkin-Katz current equation:

$$I_{Ca,L} = d \times f \times f_{Ca\text{-}entry} \times P_{Ca} \times \frac{4EF^2}{RT} \times \frac{[Ca]_i - [Ca]_o \exp(-2FE/RT)}{1 - \exp(-2FE/RT)}. \quad (2)$$

Here, d and f are voltage-dependent activation and inactivation parameters.

Eqs. 1 and 2 are the central scheme of this study. We investigate the outcome of this formulation in the framework of a standard action potential model.

Reevaluation of voltage-dependent inactivation of $I_{Ca,L}$

In the LRd model, and also in many available cardiac action potential models (DiFrancesco and Noble, 1985; Jafri et al., 1998), the voltage-dependent inactivation property was set as a major contributor of inactivation of $I_{Ca,L}$. Simple addition of a Ca^{2+} entry-dependent inactivation mechanism to the LRd model, then, would pose too much inactivation of $I_{Ca,L}$ during action potentials. Therefore, as a first step, it was necessary to reassess the voltage-dependent inactivation properties of $I_{Ca,L}$.

As shown in Fig. 1, settings for voltage-dependent inactivation properties showed large variations among different computer models. One reason for this discrepancy is that basal experimental data adopted for modeling did not necessarily discriminate Ca^{2+}-dependent inactivation from voltage-dependent inactivation properties. During experiments, Ca^{2+}-dependent inactivation is thought to be minimized or removed by using Ba^{2+}, Sr^{2+}, or monovalent cation (such as Na^+) as the charge carrier. Although Ba^{2+} is often used for this purpose, it has been recognized that Ba^{2+} allows some current-dependent inactivation (Markwardt and Nilius, 1988; Ferreira et al., 1997). There are several reports of steady-state voltage-inactivation curve for cardiac $I_{Ca,L}$, where the effect of Ca^{2+}-dependent inactivation was minimized using Na^+ as the charge carrier (often denoted as I_{ns}). These studies described inactivation curves that decrease monotonically to a nonzero value (~0.4 by Hadley and Hume, 1987; ~0.55 by Sun et al., 1997; and Linz and Meyer, 1998). We followed this type of formulation (Fig. 1 *A, thick line*):

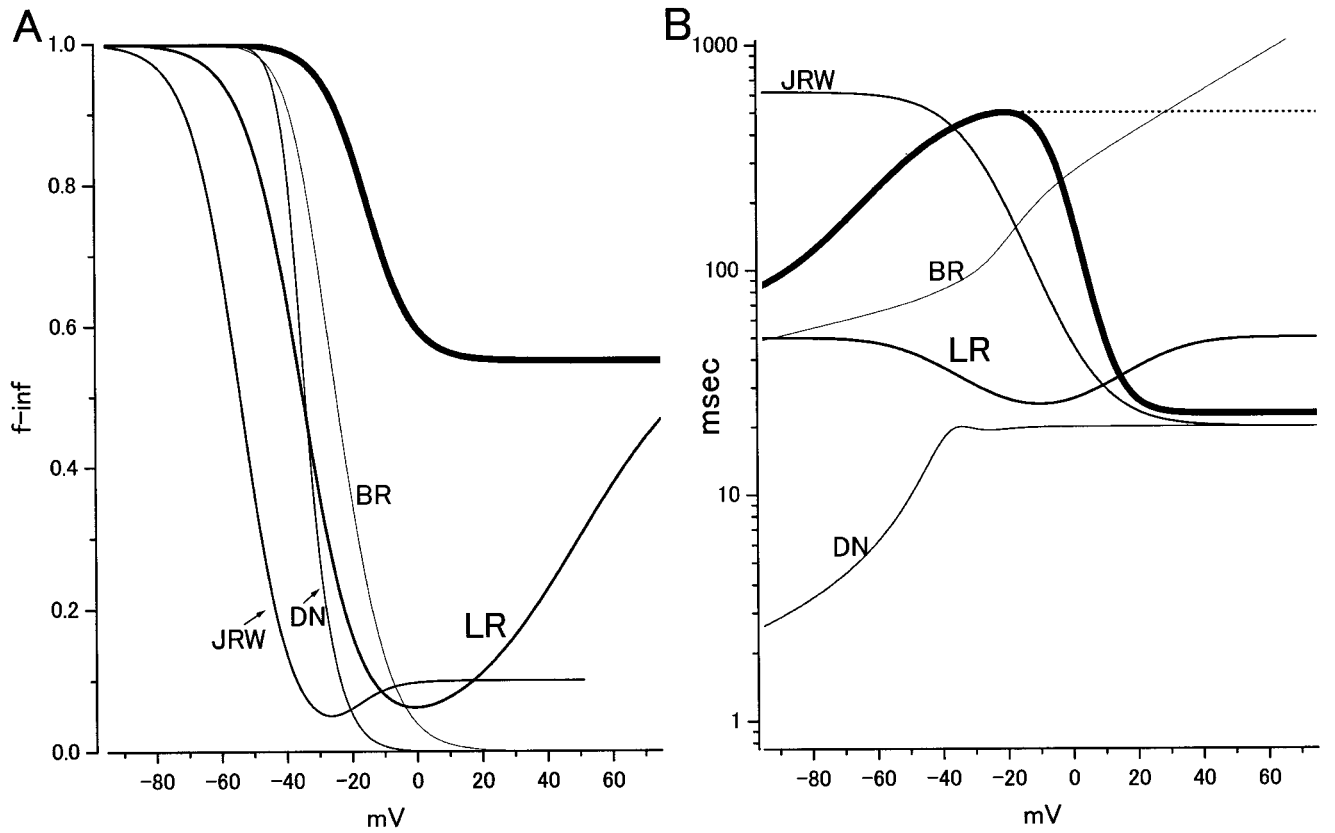

FIGURE 1 Voltage-dependent inactivation properties. (*A*) Steady state inactivation curve. (*B*) Voltage dependence of the time constant of inactivation. The formulation adopted in our Ca^{2+} entry inactivation model was shown by a thick line in *A*, and by a thick line and dotted line in *B*. Data taken from existing models are also illustrated (*BR*, Beeler and Reuter, 1977; *DN*, DiFrancesco and Noble, 1985; *LR*, Luo and Rudy, 1994; and *JRW*, Jafri et al., 1998). In *B*, a large variation in time constants of inactivation required a logarithmic scale to cover whole data.

$$f_{inf}(v) = 0.55 + 0.45/(1 + \exp((v + 15)/7)). \quad (3)$$

Available data on the time course of voltage-dependent inactivation of $I_{Ca,L}$ are complicated. In the family of voltage-gated Ca channels, voltage-dependent inactivation generally includes mechanisms with fast and slow kinetics (Hering et al., 2000). In the heart, Hadley and Hume (1987) reported that decay of Na^+ current through the L-type Ca^{2+} channel (onset of inactivation) could often be described by two exponentials. However, data showed such large variations among cells that they had to characterize the decay kinetics of I_{ns} by the half-time of inactivation to obtain consistent results. Later, Sun et al. (1997) and Mitarai et al. (2000) reported that double exponentials were required to describe the inactivation time course when test voltage was raised above 0 mV. In guinea-pig ventricular myocytes at 35°C (Mitarai et al., 2000), the time constant of the slow component was ~500 ms without apparent voltage dependence. The time constant of the fast component was shortened to ~20 ms as the test potential was elevated. Based on their Fig. 2, the amplitude of the fast component was more than two times larger at test potentials between 10 and 30 mV. They also found that the slow component dominated the inactivation when channel protein was phosphorylated. Then, slow decay observed by Linz and Meyer (1998) might be explained by the use of isoproterenol in their I_{ns} measurements.

I_{ns} data (Na^+ as the charge carrier) on recovery time course are incomplete. Hadley and Hume (1987) reported that recovery was a single exponential process with steep voltage-dependence. At −50 mV, recovery time constant was 313 ± 26 ms with Na^+ and 275 ± 26 ms with Ca^{2+} as the charge carrier. Kass and Sanguinetti (1984) used divalent cations (Ca^{2+}, Sr^{2+}, or Ba^{2+}) to study inactivation properties. In their Purkinje preparations, however, recovery time course required double exponentials when duration of the inactivating prepulse exceeded 250 ms. Recovery time constants obtained by brief prepulses, or those for fast phase of inactivation with 250-ms prepulse (which is dominant at −48 mV; see their Fig. 7) were ~50 ms at ~−50 mV. When combined with the time constant of onset of inactivation (for fast phase with Sr^{2+} or Ba^{2+} as the charge carrier), inactivation time constant showed bell-shaped voltage dependence with the peak at ~−25 mV.

Confronted by a variety and complexity of observations, we employed a practical or descriptive approach to

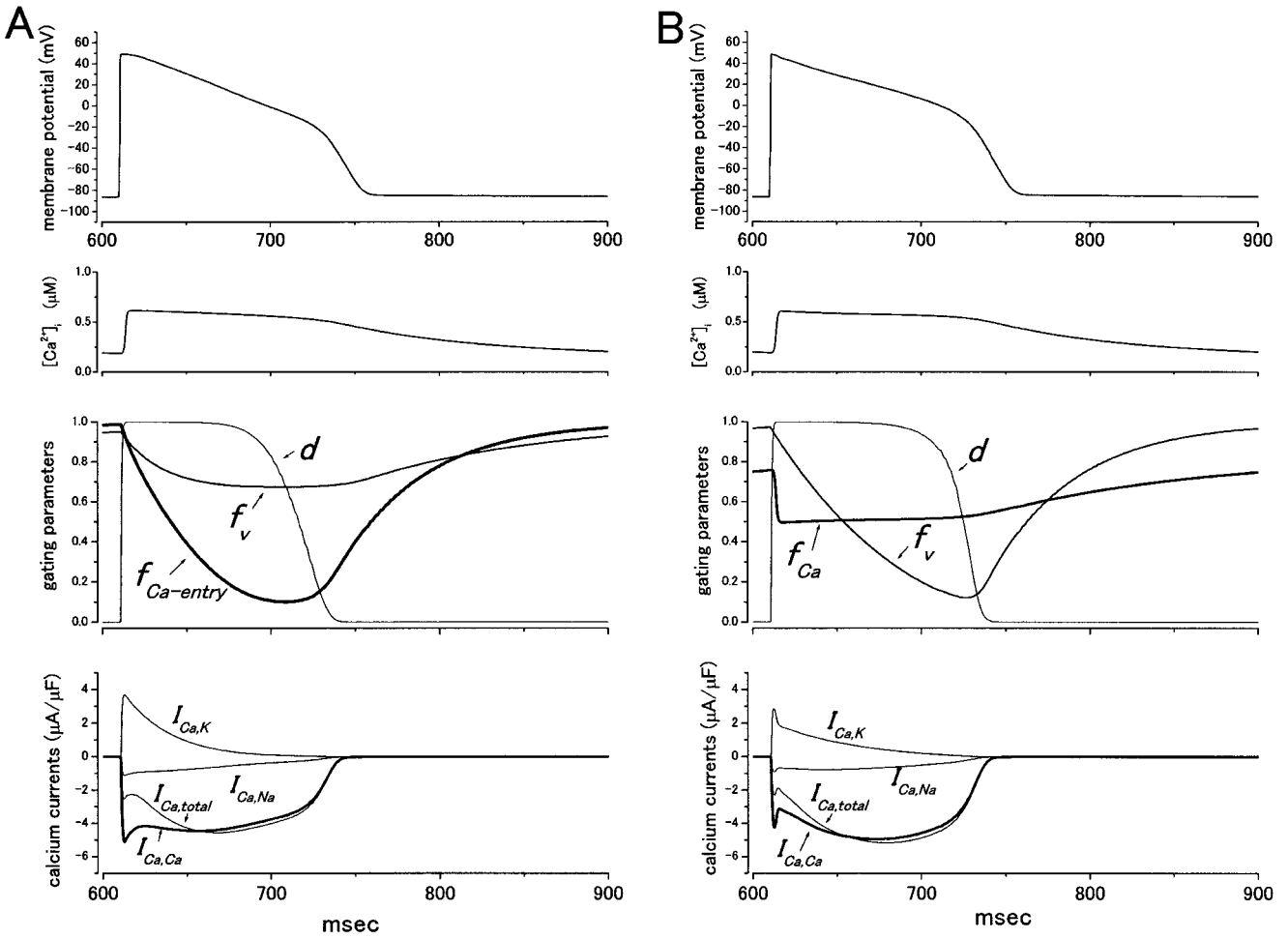

FIGURE 2 Profiles of Ca current and its gating parameters during action potential. (*A*) Model with the new formulation of Ca^{2+} entry-dependent inactivation. (*B*) The LRd model. Each column shows data obtained at the third beat of sequential stimulations delivered with a cycle length of 300 ms. The top panel shows membrane potential, the second panel Ca^{2+} transient, the third panel gating parameters, and the fourth panel Ca^{2+} current. In the third panels, thin lines show activation gate (d), medium lines show voltage-dependent inactivation gates (f_v). In *A*, f_v was shown as the weighted average of the fast and slow component ($f_{fast} \times 0.7 + f_{slow} \times 0.3$). The thick line in *A* shows the new parameter for Ca^{2+} entry-dependent inactivation ($f_{Ca\text{-}entry}$), whereas the thick line in *B* (LRd model) shows conventional Ca^{2+}-dependent inactivation parameter (f_{Ca}) as directly determined by $[Ca^{2+}]_i$ shown in the second panel. In the fourth panels, ionic currents through L-type Ca channels were shown separately depending on the charge carrier. K^+ component ($I_{Ca,K}$) and Na^+ component ($I_{Ca,Na}$) were shown by thin lines and the Ca^{2+} component, the main concern in this study, was shown by a thick line ($I_{Ca,Ca}$). Ca^{2+} entry-dependent inactivation parameter ($f_{Ca\text{-}entry}$) was equally applied to Na^+ and K^+ components of Ca current. Total Ca^{2+} current was also shown by thin lines ($I_{Ca,total}$).

implement the time course of voltage-dependent inactivation, based on guinea-pig and I_{ns} data. Inactivation is modeled with double exponential time courses although recovery follows a single exponential time course. We defined the recovery time constant combined with the fast phase of the onset of inactivation, as illustrated in Fig. 1 *B* (*thick line*).

$$\tau_{fast}(v) = 511 \times (1/(1 + \exp((-v - 48)/15)) + 0.12) \times (1/(1 + \exp((v + 5)/5)) + 0.04). \quad (4)$$

The slower phase of the onset of inactivation was assumed to have 30% of the total amplitude, and was assigned a time constant of 500 ms (Mitarai et al., 2000) at potential levels above −20 mV. This is illustrated in Fig. 1 *B* (*thick dotted line*).

The Ca^{2+} entry-dependent inactivation model

We can now go back to the central issue—the new formulation of $I_{Ca,L}$ incorporating Ca^{2+} entry-dependent inactivation defined by Eqs. 1 and 2. In this formulation, Ca^{2+}-dependent inactivation parameter (f_{Ca}) is determined by two terms: onset of inactivation proportional to the influx of Ca^{2+} (association of Ca^{2+}) and time-dependent recovery (dissociation). This proposal was implemented into the LRd model under the revised settings of voltage-dependent

inactivation as described above. Other factors to determine $I_{Ca,L}$, including voltage activation (d), the value of P_{Ca} (a permeability of Ca^{2+}), and the dynamics of intracellular Ca^{2+} were unchanged.

One of the most distinctive features of the new formulation was that changes in association and dissociation constants (α and β) greatly influenced action potential durations (APDs). Increase in α-accelerated Ca^{2+}-dependent inactivation and shortened APDs. On the other hand, increase in β decreased the extent of Ca^{2+}-inactivation and prolonged APDs. For the present, we cannot directly determine values of α and β in Eq. 1. We therefore tried to find a set of values which reproduce the experimental data of Ca^{2+}-dependent inactivation of $I_{Ca,L}$ during action potentials. It was reported that Ca^{2+}-dependent inactivation proceeded to 90–95% during the plateau phase. Later, during repolarization, $I_{Ca,L}$ recovered up to 25% (Linz and Meyer, 1998; see their Fig. 11).

Fig. 2 *A* shows a case when α is set to 0.0051 $\mu A^{-1} \times \mu F \times ms^{-1}$ and β to 0.02 ms^{-1}. With this setting, APD was almost identical with the original LRd model shown in *B*. As the plateau phase proceeds, $f_{Ca\text{-}entry}$ continues to decline to ~0.1, and then recovers. In the original LRd model (Fig. 2 *B*), decline in $I_{Ca,L}$ during action potential was produced by the voltage-dependent inactivation variable. Here, Ca^{2+}-dependent inactivation rapidly increases at the upstroke and then declines. Thus, the model produced similar temporal profile of $I_{Ca,L}$, but with different gating mechanisms.

In Fig. 3, we examined the effects of association and dissociation parameters (α and β) on the shape and durations of action potentials. It should be noted that changes in membrane permeability or maximum conductance of $I_{Ca,L}$ had little effect on APDs. Increased $I_{Ca,L}$ amplitude produced higher plateau levels initially, but was counterbalanced by entry-dependent inactivation, leaving minor and variable effects on APDs (Fig. 4 *B*). This observation was in contrast with the LRd model (Fig. 4 *A*), where the plateau height as well as APDs were modified concordantly as the maximum conductance of $I_{Ca,L}$ was altered.

Effect of Ca^{2+} released from sarcoplasmic reticulum

Ca^{2+} entering through $I_{Ca,L}$ is not the sole source for Ca^{2+}-inactivation. In our previous study, we demonstrated transient suppression of single L-type channel activity when Ca^{2+}-overloaded myocytes showed spontaneous oscillations of $[Ca^{2+}]_i$ (Hirano and Hiraoka, 1994). The most likely source of increased Ca^{2+} in this case was the sarcoplasmic reticulum (SR). It was also reported that block of Ca^{2+} release from SR by ryanodine/thapsigargin could reduce $I_{Ca,L}$ inactivation during initial 50 ms of action potentials (Linz and Meyer, 1998). These findings indicate a need to include additional Ca^{2+}-mediated inactivation mechanisms. The comprehensive modeling of intracellular Ca^{2+} handling, however, is not the purpose of the present report (see Discussion). As our primary concern was to evaluate the new formulation of Ca^{2+} entry-dependent inactivation in the framework of standard action potential model, we tried to preserve the features of the Luo-Rudy model as much as possible, and followed their intracellular Ca^{2+} dynamics. Then, to implement the effect of Ca^{2+} released from SR, we adopted the same strategy as in the case of Ca^{2+} entered through sarcolemma; Ca^{2+} released from the SR inactivates Ca channels but with different effectiveness.

We define a SR release-dependent inactivation property with a parameter $f_{Ca\text{-}SR}$, as the proportion of SR-release unaffected Ca channels (Unaffected/(Unaffected + SR-Ca inactivated)). Changes in $f_{Ca\text{-}SR}$ were determined by a term proportional to Ca^{2+}-release current from SR ($-\alpha_{SR} \times I_{rel}$) and time-dependent recovery which takes place in the proportion of SR-release modified channels ($\beta_{SR} \times (1 - f_{Ca\text{-}SR})$):

$$\frac{df_{Ca\text{-}SR}}{dt} = -\alpha_{SR} \times I_{rel} + \beta_{SR} \times (1 - f_{Ca\text{-}SR}). \qquad (5)$$

Ca^{2+}-dependent inactivation parameter in Eq. 2 now should be further reduced for the SR-release modified channels. We assumed that Ca^{2+}-dependent inactivation by the influx through $I_{Ca,L}$ and by the release from SR could be treated independently:

$$I_{Ca,L} = d \times f \times f_{Ca\text{-}entry} \times f_{Ca\text{-}SR} \times P_{Ca} \times \frac{4EF^2}{RT} \times \frac{[Ca]_i - [Ca]_o \exp(-2FE/RT)}{1 - \exp(-2FE/RT)}. \qquad (6)$$

With the values of α_{SR} and β_{SR} set to 0.05 $\mu A^{-1} \times \mu F \times ms^{-1}$ and 0.02 ms^{-1}, respectively, released Ca^{2+}-dependent inactivation rapidly increased at the upstroke of action potential and then declined slowly (Fig. 5 *A*).

Monovalent cation permeation during action potentials?

During the computation as described above, we noticed that Na^+ and K^+ permeation through the L-type Ca channel during cardiac action potentials were quite large. Many existing models, including the LRd, use a Goldman-Hodgkin-Katz formalism with large permeability for Ca^{2+} coupled with small (~1/1000) permeabilities for K^+ and Na^+. However, due to high intracellular concentration of K^+, its outward component is very large, especially following the upstroke of the action potential. This is not consistent with experimental observations that there should be no monovalent permeation while the channel is passing significant amounts of Ca^{2+} (Matsuda and Noma, 1984; Sun et al., 2000; see also Jafri et al., 1998). Therefore, we tentatively deleted the K outward current and the Na inward current component of L-type Ca channels (Fig. 5 *B*).

We then asked how these changes affect maintenance of ionic gradients across the cell membrane. The LRd model

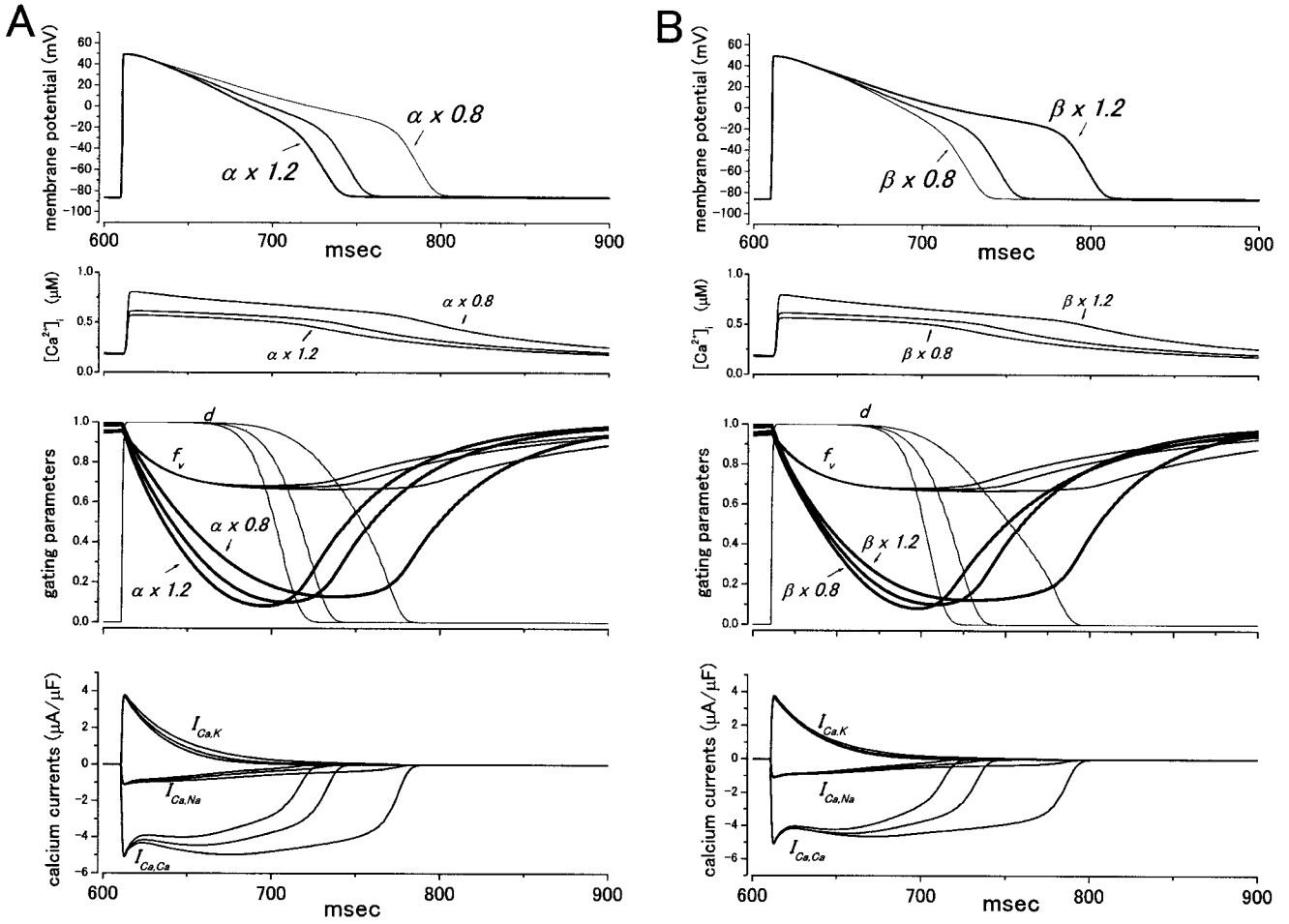

FIGURE 3 Effects of association and dissociation constants on action potential. (*A*) Effects of varied association constant (α). (*B*) Effects of varied dissociation constant (β). Method for data presentation is the same as in Fig. 2 *A* for both columns. Each panel shows superimposed data for the control and data when association constant (α, *left column*) or dissociation constant (β, *right column*) was reduced by 20% ($\times 0.8$) and increased by 20% ($\times 1.2$).

showed gradual changes in $[Na^+]_i$ and $[K^+]_i$ during long courses of stimulation. This also occurred with our monovalent cation-deleted version, with very similar gradual changes in ionic concentrations. After 200 stimulations with BCL of 300 ms, $[Na^+]_i$ increased from 9 mM to 13.0 mM in the Ca^{2+}-inactivation model without Na^+ and K^+ permeation, and to 12.2 mM in the LRd model. On the other hand, $[K^+]_i$ decreased from 141.2 mM to 136.3 mM in our Ca^{2+}-inactivation model and to 137.3 mM in the LRd model.

Voltage-clamping of Ca^{2+} entry inactivation model

We applied several voltage-clamp protocols on the model shown in Fig. 5 *B*, to further characterize and illustrate the properties of the new formulation when compared with the original LRd model.

In Fig. 6, the model was depolarized to various potential levels from the holding potential of −60 mV. Depolarization to 0 mV elicited a large inward Ca current (~5 × the amplitude that was observed during an action potential), as shown in *A*. The current initially showed rapid decay due to Ca release from SR ($f_{\text{Ca-SR}}$), followed by a slower decay mainly determined by $f_{\text{Ca-entry}}$. In the LRd model shown in *B*, this role was played by voltage-dependent inactivation, f_v. In *C*, we compared the current decay at −30, 0, and 30 mV. The speed of current decay was fastest at 0 mV where current amplitude was the largest. Fig. 6 *D* shows the peak current-voltage relationships of the new model and the LRd model. The *IV* curves were very similar between two models equipped with different inactivation properties and identical voltage-dependent activation properties of $I_{\text{Ca,L}}$.

In Fig. 7, we measured the voltage-dependent inactivation curve using a standard double-pulse protocol. Duration of conditioning was set to 1000 ms. Upper panels show current traces with the prepulse potential of −30 mV and −60 mV (holding potential). When normalized to the current amplitude obtained with prepulse potential of −80 mV (*B*), data points clearly deviated from the voltage-dependent inactivation curve defined by equation 3 ($f_{\text{inf}}(v)$). Records

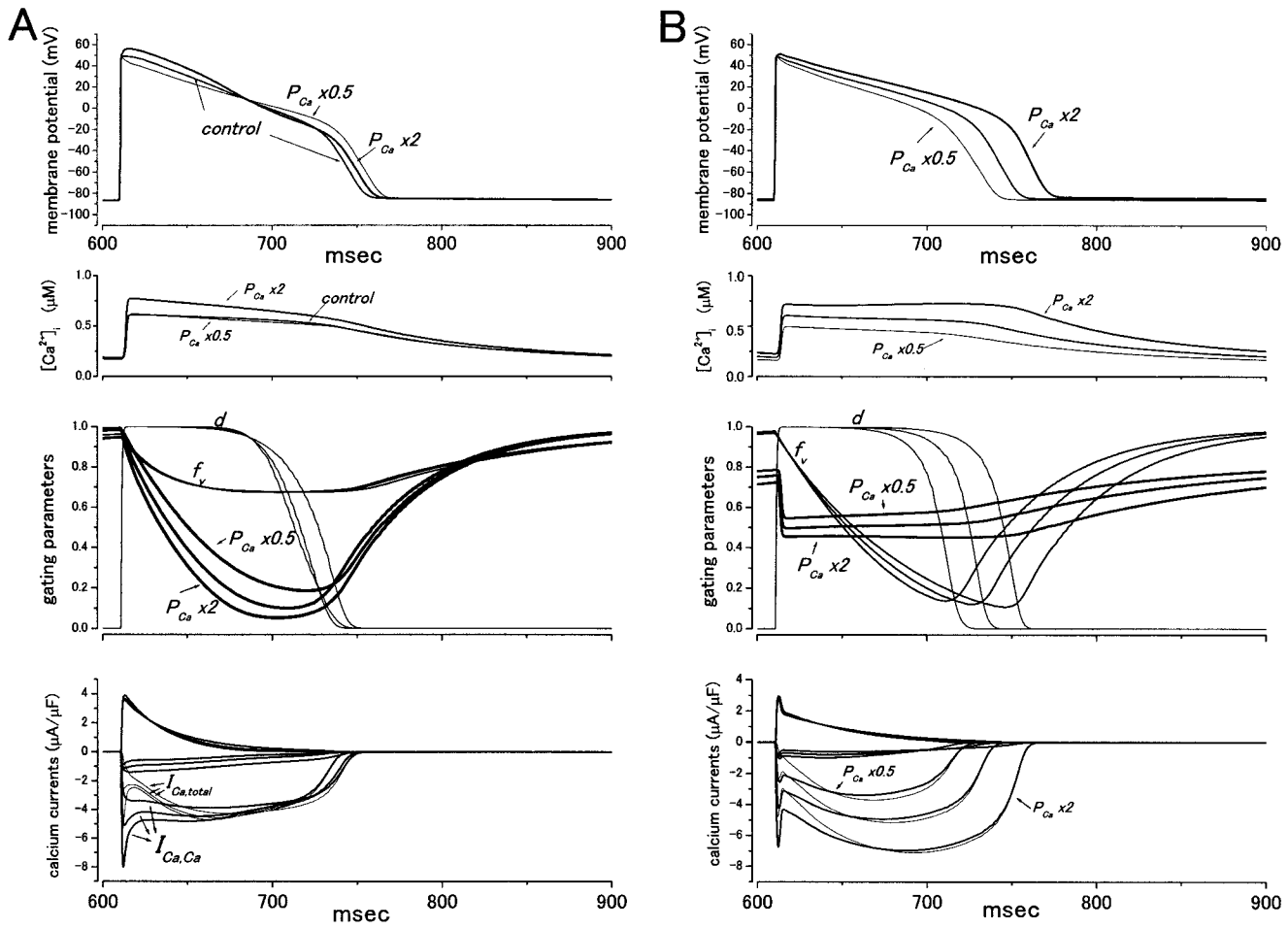

FIGURE 4 Effects of membrane permeability of Ca^{2+} on action potential. (*A*) Model with the new formulation of Ca^{2+} entry-dependent inactivation. (*B*) The LRd model. Method for data presentation is the same as in Fig. 2. Each panel shows superimposed data for the control and data when P_{Ca} was reduced by half ($P_{Ca} \times 0.5$) and doubled ($P_{Ca} \times 2$).

of gating parameters shown in *A* indicated that decrease in current amplitude at −30 mV was mainly brought by $f_{Ca\text{-entry}}$. These results are completely different from the LRd model (*C*), where observed points closely followed the "pure" voltage-inactivation curve $f_{inf}(v)$.

In Fig. 8 *A*, we compared the responses to train of depolarizing pulses in voltage-clamp mode (*upper panel*) and to repetitive stimulation in current-clamp mode (*lower panel*). In each panel, the model was initially depolarized (stimulated) at 2 Hz for 12 s. The frequency was then transiently increased to 3 Hz, before subsequent return to 2 Hz. In voltage-clamp mode (*upper panel*), when pacing frequency was increased, a transient suppression of peak Ca^{2+} transient was followed by an augmentation toward a new steady level. Upon a reduction of pacing frequency, peak Ca^{2+} transient declined after a transient increase. This behavior was essentially the same with trains of action potentials (*lower panel*), although recovery of peak Ca^{2+} transient was slow following the increase upon reduction of pacing frequency to 2 Hz. The same protocol was applied to the LRd model (Fig. 8 *B*). The two models equipped with identical properties of CICR responded with almost identical behavior, except that the amplitude of Ca^{2+} transient was higher in our new model. Also, the level of Ca^{2+} concentration in network sarcoplasmic reticulum (NSR) reached higher level during trains of stimulations.

Behavior during prolonged APDs

Prolongation of APD is an important substrate for clinical arrhythmias (Chiang and Roden, 2000). In long QT syndromes, this is brought about by a decreased K current amplitude or increased Na current during the plateau, due to the mutation of channel proteins. Using the model shown in Fig. 5 *B*, we next examined how the reduction of I_{Kr} and I_{Ks} current modulate the action potentials and the profiles of $I_{Ca,L}$.

As shown in Fig. 9 *A*, *b* and *c*, reduction of K currents in the new model prolonged APDs and induced early afterdepolarization (EADs). During the plateau phase where EADs took place, not only voltage inactivation but also

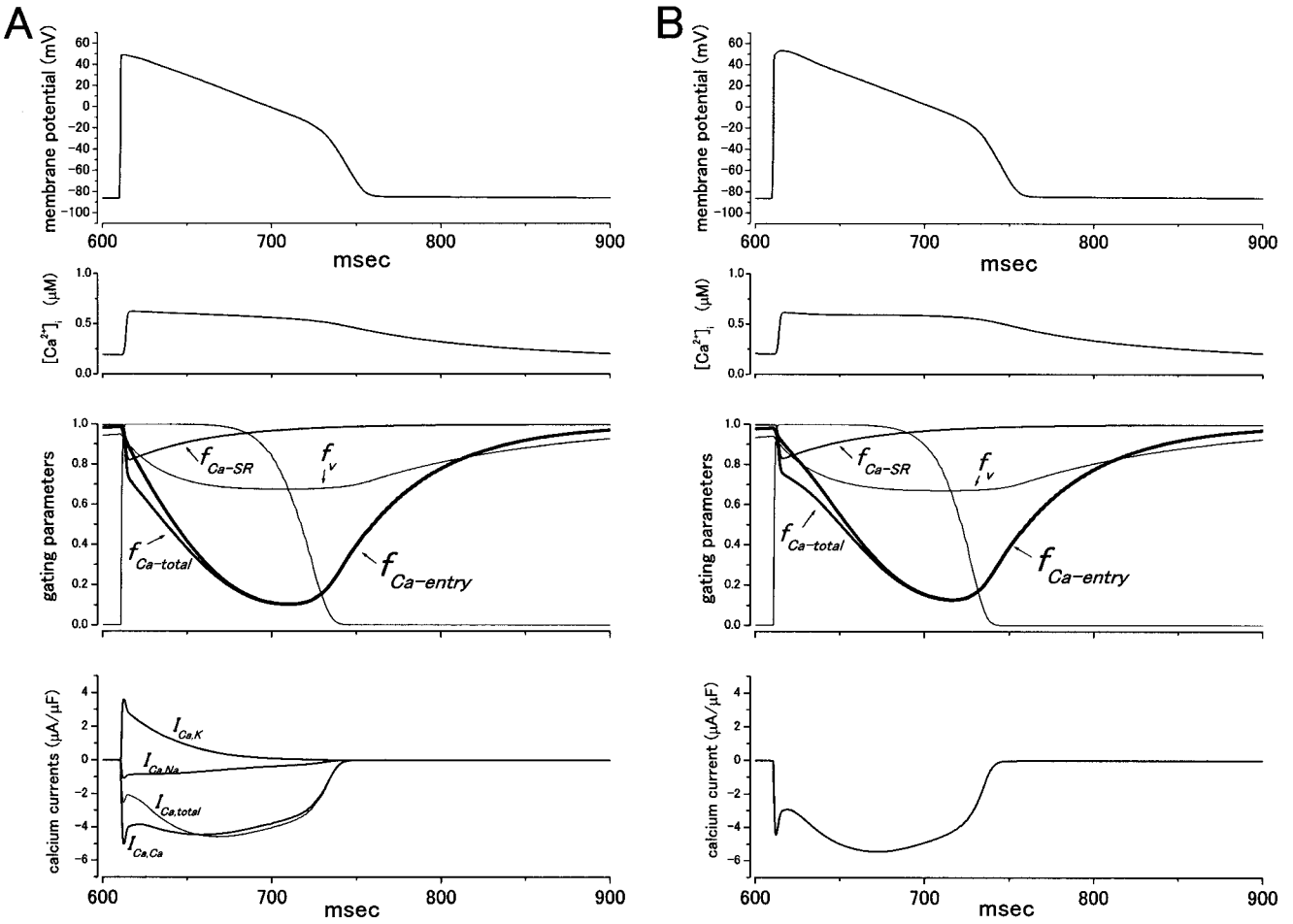

FIGURE 5 (*A*) Inactivation caused by Ca^{2+} released from SR. (*B*) Effect of the removal of monovalent cation permeation. To obtain APDs similar to the original LRd model (Fig. 2 *B*), the value of association rate constant (α, see Eq. 1) was set to 0.0041 $\mu A^{-1} \times \mu F \times ms^{-1}$ in *B*. Value of dissociation constant (β in Eq. 1) was left unchanged (0.02 ms^{-1}). Method for data presentation is the same as in Fig. 2 *A* for both columns. In the third panel, the thick line shows the parameter for Ca^{2+} entry-dependent inactivation ($f_{Ca\text{-}entry}$), whereas the medium-width line shows the parameter for SR-release dependent inactivation ($f_{Ca\text{-}SR}$). The product of these parameters, which indicates total Ca^{2+}-dependent inactivation ($f_{Ca\text{-}total}$), is also illustrated.

Ca^{2+}-dependent inactivation was incomplete. As determined by the balance of inward and outward current, membrane potentials oscillate with prominent changes in activation parameters (activation and deactivation). EADs were also accompanied by changes in Ca^{2+} entry-dependent inactivation parameter ($f_{Ca\text{-}entry}$).

We compared these results with the behavior of the original Luo-Rudy models (Fig. 9 *B*). In the downloaded version of the LRd model (corresponding to the endocardial cell in Viswanathan et al., 1999), reduction of I_{Kr} alone failed to produce EADs. However, reduction of I_{Ks} below 30% produced EADs or failure of repolarization. In Fig. 9 *B*, *c* where I_{Ks} was reduced to 25% of the control, EADs appeared without appreciable changes in Ca^{2+}-dependent inactivation parameter (f_{Ca}).

Prolongation of APDs can be produced also by changes in $I_{Ca,L}$ parameters. As shown in Fig. 3, changes in association and dissociation constants of Ca^{2+} and the channel protein (α and β) were the most efficient way in Ca^{2+}-inactivation models. When EADs were produced by reducing α by 30% (Fig. 9 *A*, *d*), profiles of gating parameters underlying the EADs were surprisingly similar with the cases produced by reduced K-current amplitudes.

DISCUSSION

By adopting a very simple formulation of Ca^{2+}-dependent inactivation, we reconstructed the behavior of $I_{Ca,L}$ during cardiac action potentials. The gating parameter to determine Ca^{2+} entry-dependent inactivation ($f_{Ca\text{-}entry}$) gradually declined to ~0.1 during the plateau phase and recovered up to ~0.3 at final repolarization. Our results support the view that Ca^{2+} entry-dependent inactivation can play a significant role to determine the time course of L-type Ca current during cardiac action potentials, consistent with recent experimental findings (Sun et al., 1997; Linz and Meyer, 1998; Alseikhan et al., 2002).

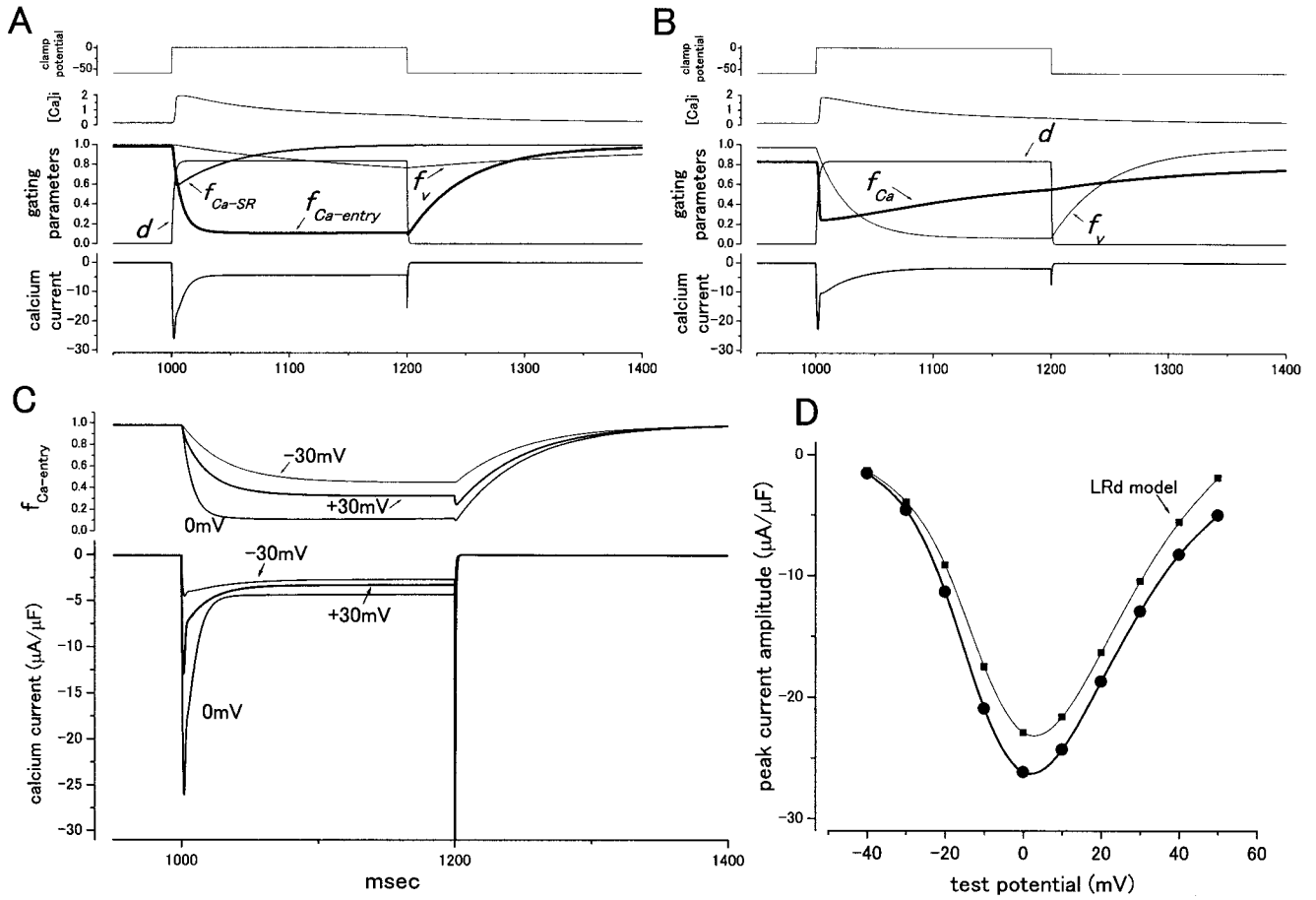

FIGURE 6 Voltage dependence of current decay and the peak IV relationships. (*A*) Voltage clamp record of the model with the new formulation of Ca^{2+} entry-dependent inactivation. (*B*) Voltage clamp record of the LRd model. Method for data presentation is the same as in Fig. 2. In this and subsequent figures, *calcium current* in the LRd model represents total current including Na^+ and K^+ components. In both cases, the models were depolarized to 0 mV for 200 ms after holding at −60 mV for 1000 ms. (*C*) Voltage dependence of current decay in the new Ca^{2+}-inactivation model. Three superposed traces for $f_{Ca\text{-}entry}$ and calcium current obtained at +30, 0, and −30 mV were shown. (*D*) Peak inward current-voltage relationships. Large closed circles are for the new model and small squares for the LRd model.

Comparison with the LRd model

In this study, we replaced the I_{Ca} subsystem in the LRd model. The new gating mechanisms resulted in several important properties not simulated in the LRd model, while leaving some basic properties untouched.

In our formulation (Fig. 3), APDs were greatly affected by the alteration of binding efficacy between Ca^{2+} ion and the Ca channel (actually through calmodulin constitutively tethered to channel protein; see below). Recently, prominence of Ca^{2+}-dependent inactivation of L-type Ca channels in controlling APDs was experimentally demonstrated by the expression of a Ca^{2+}-insensitive mutant calmodulin, which virtually eliminated Ca^{2+}-dependent inactivation and strikingly prolonged APDs (Alseikhan et al., 2002). On the other hand, changes in maximum conductance or P_{Ca} had small and variable effects on APDs in a standard condition (Fig. 4). This is in contrast to the original LRd model.

During voltage clamp simulations, peak *IV* relationships were kept almost identical (Fig. 6). However, mechanisms to determine the voltage-dependent inactivation curve were completely different between the two models (Fig. 7). In the present model, inactivation curve with a minimum ~0 mV was not built into model equations, but emerged from Ca^{2+} entry-dependent inactivation.

Intracellular Ca^{2+} dynamics and the modulation of Ca current

In the present study, CICR or dynamics of intracellular Ca^{2+} affects $I_{Ca,L}$ through the parameter $f_{Ca\text{-}SR}$, as determined by the amplitude of Ca^{2+}-release from SR (I_{rel}). Experimental findings indicate that the effect of SR release is particularly important during the initial ~50 ms of action potentials (Linz and Meyer, 1998) or during

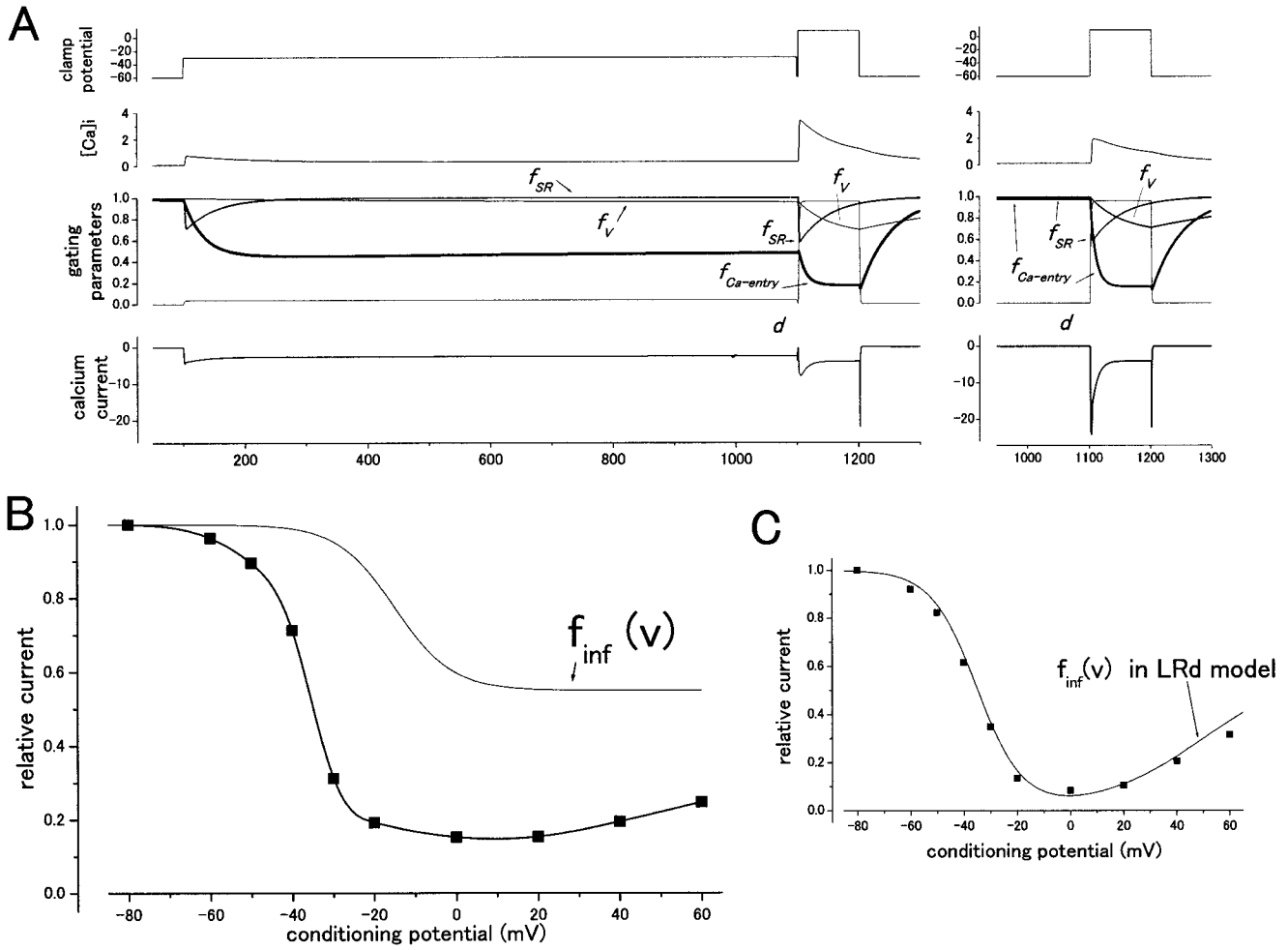

FIGURE 7 Measurement of the voltage-dependent inactivation curve. (*A*) Current traces. The model with the new formulation was depolarized to −30 mV for 1000 ms (*left column*) or held at −60 mV (*right column*) before test pulses to +10 mV were applied. The conditioning pulses were separated by a gap of 2 ms at the holding potential of −60 mV. Method for data presentation is the same as in Fig. 2 *A*. (*B*) Inactivation curve in the new model. The peak inward current obtained at the test pulse was normalized by its maximal value and was plotted against prepulse potential. Voltage-dependent inactivation curve presented in Fig. 1 *A* was also shown by a thin line (f_{inf}(v)). (*C*) Inactivation curve obtained in the LRd model using the identical protocol. Voltage-dependent inactivation curve presented in Fig. 1 *A* (*LR*) was superposed on data points.

depolarizing pulses in voltage clamp experiments using conventional square pulses (Sun et al., 1997). Although our new model is consistent with these studies, significant issues remain to be examined concerning the effects evoked by intracellular Ca^{2+} dynamics.

The LRd model generates action potentials through detailed description of current systems. However, its Ca^{2+} handling subsystem is very simple and phenomenological. As in the DiFrancesco-Noble model (1985), the LRd model has a single cytosolic Ca^{2+} compartment (common pool) to which both Ca^{2+} influx through $I_{Ca,L}$ and SR Ca^{2+} release are directed. In cardiac myocytes, SR Ca^{2+} release is proportional to the influx of trigger Ca^{2+} (graded response) whereas released Ca^{2+} from SR is significantly larger than the trigger influx (high gain). It is difficult to accommodate "graded response" and "high gain" simultaneously in common pool models, because a high-gain system generally leads to all-or-none–type regenerative Ca^{2+} releases (Stern, 1992). In the LRd model, Ca^{2+} release is a function of Ca^{2+} influx through the sarcolemma, but independent of Ca^{2+} release from the SR. In this setting, released Ca^{2+} may have a suppressive effect on CICR because it reduces the concentration gradient of Ca^{2+} between the common pool and the junctional SR. The formulation of CICR employed here does not include regenerative Ca^{2+} release, a mechanism that admittedly is not biophysically accurate.

Recent local control theory established that CICR is determined by local Ca^{2+} dynamics (such as Ca^{2+} sparks), not by the average $[Ca^{2+}]_i$ within the myocytes (Wier and Balke, 1999; Wang et al., 2001). For example, Wier et al. (1994) observed that gain of CICR (the ratio of released Ca^{2+} to influx of Ca^{2+} through the channel) is dependent on the voltage of clamp pulses, with the highest gain at ~−20 mV. This observation arises from the fact that the amplitude

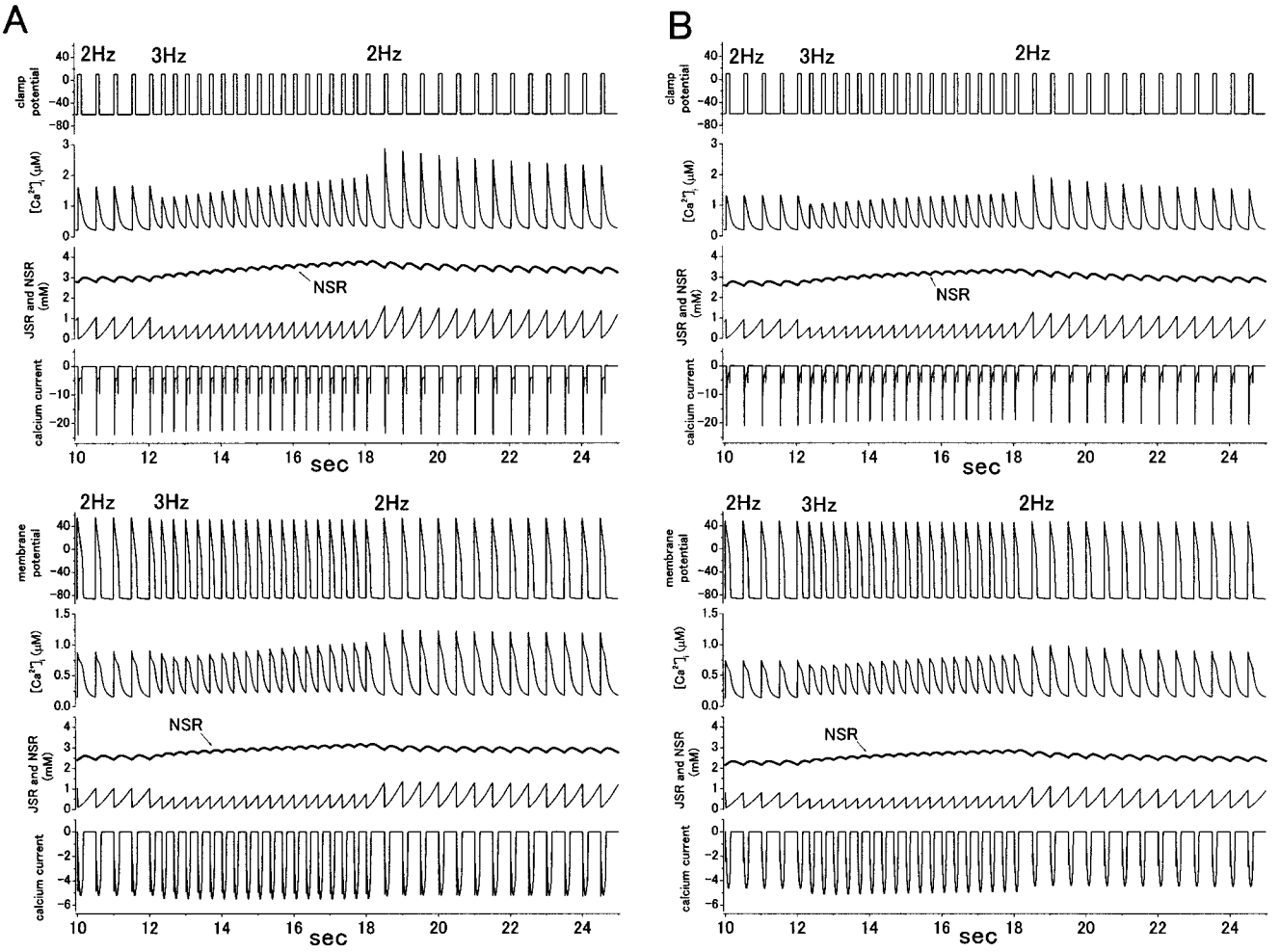

FIGURE 8 Effects of trains of stimulation. (*A*) Data from the new Ca^{2+} entry-dependent inactivation model. (*B*) Data from the LRd model. In each column, upper panels show data obtained by voltage clamping to +10 mV with a frequency indicated at the top. Lower panels show the effect of trains of stimulation delivered in a identical way as in voltage clamp experiments. Method for data presentation is the same as in Fig. 2, except that in the third panels, Ca^{2+} concentrations of junctional SR (*JSR*) and network SR (*NSR*) are shown.

of unitary Ca channel current is high near threshold levels (located far from the reversal potential of Ca^{2+}), and therefore is more effective to trigger Ca^{2+} sparks or release of Ca^{2+} from SR. These important properties of CICR could not be reproduced in the LRd model and accordingly, in our present model which faithfully followed the formulation presented in the LRd model. During rapid stimulations (Fig. 8), the new formulation of $I_{Ca,L}$ inactivation increased the amplitude of Ca transient and slightly raised the level of NSR Ca^{2+} concentration. It did not, however, affect the basic properties of intracellular Ca^{2+} dynamics.

There are now several models of intracellular Ca^{2+} handling with more complex structures and detailed description of Ca^{2+}-induced Ca^{2+} release. For example, Rice, et al. (1999) introduced stochastic methods to make a robust model with high gain and graded Ca^{2+} release in the functional unit of the cardiac dyadic space, whereas Stern et al. (1999) stressed the importance of allosteric interactions between ryanodine receptors. To extend the range of phenomena to be evaluated, it is necessary to incorporate a more detailed intracellular Ca^{2+} handling system into cardiac action models.

In the heart, Ca channel is not the sole current system modulated by $[Ca^{2+}]_i$. Additional Ca^{2+}-modified channels or ion-transporters include not only Na^+–Ca^{2+} exchanger and I_{Ks} potassium channel, but also Na channel (Tan et al., 2002). If the localization or distribution of channel proteins is not uniform with respect to local Ca^{2+} distribution in the myocyte, modeling of $[Ca^{2+}]_i$ effect on channel function should be highly complicated.

Further revisions required

Several important modulatory functions are not implemented in this version of Ca current formulation, in addition to the problems related to handling of $[Ca^{2+}]_i$. Ca channel open probability was potentiated following large

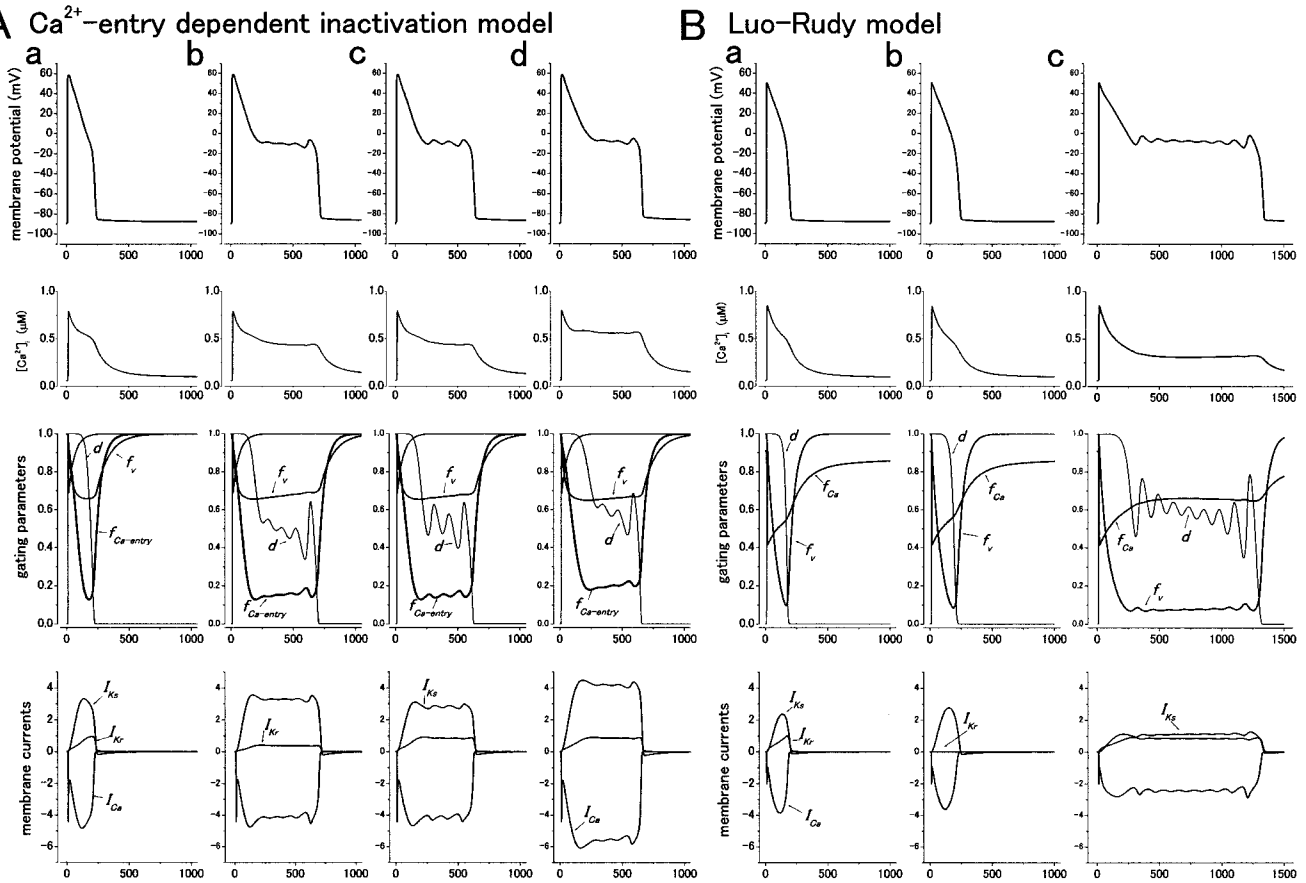

FIGURE 9 Prolongation of APDs and the profile of Ca current. Left four columns (*A, a–d*) show data from the model with the new formulation of Ca^{2+} entry-dependent inactivation. Right three columns (*B, a–c*) show data from the LRd model. Each column shows data obtained at the first beat of sequential stimulations delivered with a cycle length of 1200–2000 ms. Method for data presentation is the same as in Fig. 2, except that in the fourth panels, current amplitudes for I_{Ks}, I_{Kr}, and I_{Ca} (total amplitude) are shown. In *A*, the first column (*a*) is the control, the second column (*b*) was obtained by reducing amplitude of I_{Kr} by 55%, the third column (*c*) was obtained by reducing I_{Ks} amplitude by 20%, and the fourth column (*d*) was obtained by reducing the association constant of Ca^{2+} and Ca channel (α) by 30%. In *B* (LRd model), the first column (*a*) is the control, the second column (*b*) was obtained by totally removing I_{Kr}, and the third column (*c*) was obtained by reducing I_{Ks} amplitude to 25%.

depolarization. In contrast to the case in skeletal muscle (Hulme et al., 2002), prepulse facilitation in cardiac myocytes may involve a mechanism related to voltage-dependent conformational change (Hirano et al., 1999). Modulation of $I_{Ca,L}$ by Ca^{2+} include potentiation when increase in $[Ca^{2+}]_i$ was modest (Hirano and Hiraoka, 1994). The latter effect is linked to phosphorylation of the channel protein by Ca^{2+} calmodulin-dependent kinase II, and is an example of pivotal roles of Ca^{2+} as the modulator of various enzyme activities.

Computational modeling is an important companion to experimental work, systematizing existing experimental observations and serving as a predictable tool for further experimental investigation. However, the model is only as accurate as the quality of the experimental data used in its development. As new experimental insight becomes available, models must be reassessed and revised.

Addendum: After the original manuscript was submitted, a set of papers appeared describing how β-adrenergic stimulation modulates Ca^{2+}- and voltage-dependent inactivation, including their relative contributions (Findlay, 2002a,b). Their voltage-inactivation curve was similar to that used in this study, when myocytes were under β-adrenergic stimulation.

REFERENCES

Alseikhan, B. A., H. M. Colecraft, C. D. DeMaria, and D. T. Yue. 2002. Prominence of Ca^{2+}-dependent inactivation of L-type Ca channels in controlling cardiac action potential duration. *Biophys. J.* 82:358a (Abstr.).

Beeler, G. W., and H. Reuter. 1977. Reconstruction of the action potential of ventricular myocardial fibres. *J. Physiol.* 268:177–210.

Bers, D. M., and E. Perez-Reyes. 1999. Ca channels in cardiac myocytes: structure and function in Ca influx and intracellular Ca release. *Cardiovasc. Res.* 42:339–360.

Chiang, C.-E., and D. M. Roden. 2000. The long QT syndrome: Genetic basis and clinical implications. *J. Am. Coll. Cardiol.* 36:1–12.

Clancy, C. E., and Y. Rudy. 2001. Cellular consequences of HERG mutations in the long QT syndrome: precursors to sudden cardiac death. *Cardiovasc. Res.* 50:301–313.

DiFrancesco, D., and D. Noble. 1985. A model of cardiac electrical activity incorporating ionic pumps and concentration changes. *Philos. Trans. R. Soc. Lond.* 307:353–398.

Eckert, R., and J. E. Chad. 1984. Inactivation of Ca channels. *Prog. Biophys. Mol. Biol.* 44:215–267.

Faber, G. M., and Y. Rudy. 2000. Action potential and contractility changes in $[Na^+]_i$ overloaded cardiac myocytes: a simulation study. *Biophys. J.* 78:2392–2404.

Ferreira, G., J. Yi, E. Ríos, and R. Shirokov. 1997. Ion-dependent inactivation of barium current through L-type calcium channels. *J. Gen. Physiol.* 102:1005–1030.

Findlay, I. 2002a. Voltage- and cation-dependent inactivation of L-type Ca^{2+} channel currents in guinea-pig ventricular myocytes. *J. Physiol.* 541:731–740.

Findlay, I. 2002b. β-Adrenergic stimulation modulates Ca^{2+}- and voltage-dependent inactivation of L-type Ca^{2+} channel currents in guinea-pig ventricular myocytes. *J. Physiol.* 541:741–751.

Hadley, R. W., and J. R. Hume. 1987. An intrinsic potential-dependent inactivation mechanism associated with calcium channels in guinea-pig myocytes. *J. Physiol.* 389:205–222.

Hering, S., S. Berjukow, S. Sokolov, R. Marksteiner, R. G. Weisz, R. Kraus, and E. N. Timin. 2000. Molecular determinants of inactivation in voltage-gated Ca^{2+} channels. *J. Physiol.* 582:237–249.

Hirano, Y., and M. Hiraoka. 1994. Dual modulation of unitary L-type Ca^{2+} channel currents by $[Ca^{2+}]_i$ in fura-2-loaded guinea-pig ventricular myocytes. *J. Physiol.* 480:449–463.

Hirano, Y., and M. Hiraoka. 2001. Ca^{2+}-entry dependent inactivation of cardiac L-type Ca current: a novel formulation for computer model of cardiac action potential. *Jpn. J. Physiol.* 51(Suppl.):S149 (Abstr.).

Hirano, Y., T. Yoshinaga, M. Murata, and M. Hiraoka. 1999. Prepulse-induced mode 2 gating behavior with and without β-adrenergic stimulation in cardiac L-type Ca channels. *Am. J. Physiol.* 176(*Cell Physiol. 45*):C1338–C1345.

Hulme, J. T., M. Ahn, S. D. Hauschka, T. Sheuer, and W. A. Catterall. 2002. A novel leucine zipper targets AKAP15 and cyclic AMP-dependent protein kinase to the C terminus of the skeletal muscle Ca^{2+} channel and modulates its function. *J. Biol. Chem.* 277:4079–4087.

Jafri, M. S., J. J. Rice, and R. L. Winslow. 1998. Cardiac Ca^{2+} dynamics: the roles of ryanodine receptor adaptation and sarcoplasmic reticulum load. *Biophys. J.* 74:1149–1168.

Kass, R. S., and M. C. Sanguinetti. 1984. Inactivation of calcium channel current in the calf cardiac Purkinje fiber. Evidence for voltage- and calcium-mediated mechanisms. *J. Gen. Physiol.* 84:705–726.

Linz, K. W., and R. Meyer. 1998. Control of L-type calcium current during the action potential of guinea-pig ventricular myocytes. *J. Physiol.* 513:425–442.

Luo, C. H., and Y. Rudy. 1994. A dynamic model of the cardiac ventricular action potential. I. simulations of ionic currents and concentration changes. *Circ. Res.* 74:1071–1096.

Markwardt, F., and B. Nilius. 1988. Modulation of calcium channel currents in guinea-pig single ventricular heart cells by the dihydropyridine Bay K 8644. *J. Physiol.* 399:559–575.

Matsuda, H., and A. Noma. 1984. Isolation of calcium current and its sensitivity to monovalent cations in dialysed ventricular cells of guinea-pig. *J. Physiol.* 357:553–573.

McDonald, T. F., S. Pelzer, W. Trautwein, and D. J. Pelzer. 1994. Regulation and modulation of calcium channels in cardiac, skeletal and smooth muscle cells. *Physiol. Rev.* 74:365–507.

Mitarai, S., M. Kaibara, K. Yano, and K. Taniyama. 2000. Two distinct inactivation processes related to phosphorylation in cardiac L-type Ca^{2+} channel currents. *Am. J. Physiol. Cell Physiol.* 279:C603–C610.

Nakajima, T., T. Furukawa, Y. Hirano, T. Tanaka, H. Sakurada, T. Takahashi, R. Nagai, T. Itoh, Y. Katayama, Y. Nakamura, and M. Hiraoka. 1999. Voltage-shift of current activation in HERG S4 mutation (R534C) in LQT2. *Cardiovasc. Res.* 44:283–293.

Peterson, B. Z., C. D. DeMaria, and D. T. Yue. 1999. Calmodulin is the Ca^{2+} sensor for Ca^{2+}-dependent inactivation of L-type calcium channels. *Neuron.* 22:549–558.

Rice, J. J., M. S. Jafri, and R. L. Winslow. 1999. Modeling gain and gradedness of Ca^{2+} release in the functional unit of the cardiac dyadic space. *Biophys. J.* 77:1871–1884.

Stern, M. D. 1992. Theory of excitation-contraction coupling in cardiac muscle. *Biophys. J.* 63:497–517.

Stern, M. D., L.-S. Song, H. Cheng, J. S. K. Sham, H. T. Yang, K. R. Boheler, and E. Ríos. 1999. Local control models of cardiac excitation-contraction coupling. A possible role for allosteric interactions between ryanodine receptors. *J. Gen. Physiol.* 113:469–489.

Sun, L., J.-S. Fan, J. W. Clark, and P. T. Palade. 2000. A model for the L-type Ca^{2+} channel in rat ventricular myocytes: ion selectivity and inactivation mechanisms. *J. Physiol.* 529:139–158.

Sun, H., N. Leblanc, and S. Nattel. 1997. Mechanisms of inactivation of L-type calcium channels in human atrial myocytes. *Am. J. Physiol.* 272(*Heart Circ. Physiol. 41*): H1625–H1635.

Tan, H. L., S. Kupershmidt, R. Zhang, S. Stepanovic, D. M. Roden, A. A. M. Wilde, M. E. Anderson, and J. R. Balser. 2002. A calcium sensor in the sodium channel modulates cardiac excitability. *Nature.* 415:442–447.

Viswanathan, P. C., R. M. Shaw, and Y. Rudy. 1999. Effects of I_{Kr} and I_{Ks} heterogeneity on action potential duration and its rate dependence. A simulation study. *Circulation.* 99:2466–2474.

Wang, S.-Q., L.-S. Song, E. G. Lakatta, and H. Cheng. 2001. Ca^{2+} signaling between single L-type Ca^{2+} channels and ryanodine receptors in heart cells. *Nature.* 410:592–596.

Wier, W. G., and C. W. Balke. 1999. Ca release mechanism, Ca sparks and local control of excitation-contraction coupling in normal heart muscle. *Circ. Res.* 85:770–776.

Wier, W. G., T. M. Eagan, J. R. Lopez-Lopez, and C. W. Balke. 1994. Local control of excitation-contraction coupling in rat heart cells. *J. Physiol.* 474:463–471.

Zeng, J., K. R. Laurita, D. S. Rosenbaum, and Y. Rudy. 1995. Two components of the delayed rectifier K^+current in ventricular myocytes of the guinea pig type: Theoretical formulation and their role in repolarization. *Circ. Res.* 77:140–152.

Zuhlke, R. D., G. S. Pitt, K. Deisseroth, R. W. Tsien, and H. Reuter. 1999. Calmodulin supports both inactivation and facilitation of L-type calcium channels. *Nature.* 399:159–162.